

UNIL-TP-5/95
 BA-95-17
 hep-ph/9512345

Radiative Electroweak Breaking with Pseudogoldstone Higgs Doublets

B. Ananthanarayan¹

Institut de Physique Théorique, Université de Lausanne,
 CH-1015 Lausanne, Switzerland

Q. Shafi

Bartol Research Institute, University of Delaware
 Newark, DE 19716, USA

Abstract

We consider a realistic example of supersymmetric grand unification based on $SU(3)_c \times SU(3)_L \times SU(3)_R$ in which the electroweak (EW) higgs doublets are ‘light’ as a consequence of the ‘pseudogoldstone’ mechanism. We discuss radiative EW breaking in this model, exploring in particular the ‘small’ (order unity) and ‘large’ ($\approx m_t/m_b$) $\tan \beta$ regions by studying the variations of r ($\equiv \sqrt{\mu_{1,2}^2/\mu_3^2}$), where $\mu_{1,2,3}^2$ are the well known MSSM parameters evaluated at the GUT scale. For r sufficiently close to unity the quantity $\tan \beta$ can be of order unity, but the converse is not always true.

¹Present address: Institut für Theoretische Physik, Universität Bern, CH 3012, Bern, Switzerland

1 Introduction

Understanding how the electroweak higgs doublets of the minimal supersymmetric standard model (MSSM) remain ‘light’ ($\sim 10^2 GeV$) within the framework of supersymmetric grand unified theories (SUSY GUTS) poses an important challenge for model builders. In supersymmetric trinification with gauge group $G \equiv SU(3)_c \times SU(3)_L \times SU(3)_R$, by imposing suitable discrete symmetries for instance, it is possible to protect the EW doublets from becoming superheavy without fine tuning [1]. The supersymmetric μ -term of MSSM arises from a higher order (non-renormalizable) term in the superpotential. This approach leads to a number of testable predictions. The proton turns out to be essentially stable, while the MSSM parameter $\tan \beta \approx m_t/m_b$. It is interesting to recall that in this case, by fixing $m_b(m_b) = 4.25 \pm 0.10$ GeV and $\alpha_s(M_z) = 0.12 \pm 0.01$, the top quark mass was predicted [2] to lie in a range which is in very good agreement with the subsequent CDF/DO measurements.

A somewhat different approach for obtaining the light doublets relies on the idea of an accidental ‘pseudo-symmetry’ [3] which is spontaneously broken. [It also may be broken both explicitly as well as by radiative corrections.] Examples [4,5] based on $SU(6)$ ($SU(5)$ and $SO(10)$ do not seem to work) and more recently [6] on $G(\equiv (SU(3))^3)$ have been presented. In this paper we wish to focus on the pseudogoldstone mechanism in G and study the implications of merging it with the radiative EW breaking scenario. In section 2 we provide the details of this mechanism within the framework of G . What partially distinguishes this example from some previous work based on $SU(6)$

can be explained in terms of the parameter $r \equiv \sqrt{\mu_1^2/\mu_3^2}$ ($\equiv \sqrt{\mu_2^2/\mu_3^2}$), where $\mu_1^2, \mu_2^2, \mu_3^2$ are the well known mass squared parameters of the tree level scalar potential of MSSM, evaluated at the GUT scale M_G . In the simplest $SU(6)$ model r is equal to unity, up to corrections of order $(1TeV/M_G)^2$, where 1 TeV specifies the supersymmetry breaking scale. In the $(SU(3))^3$ case, r deviates from unity even in the supersymmetric limit due to the presence of a superpotential term which breaks pseudosymmetry at tree level. Nonetheless, this leads to the desired higgs doublets [6]. Indeed, in the absence of this additional term r is unity, but then the top quark turns out to be massless at tree level which is unacceptable. In section 3 we consider radiative EW breaking as well as the ensuing sparticle spectroscopy, focusing on r very close to unity such that $\tan \beta$ is of order unity. We find interesting constraints on the parameters, namely $|M_{1/2}| \lesssim m_0 \lesssim |A|$, where $M_{1/2}(m_0)$ denote the universal gaugino (scalar) mass, and A is the universal trilinear scalar coupling. Figures 1-6 highlight this region of the parameter space. In Figs. 7-10 we show how by varying the ratio A/m_0 , the quantity $r \gg 1$ without $\tan \beta$ becoming large. In section 4 we briefly summarize the large $\tan \beta$ case obtained by varying r further away from unity (Fig. 11).

2 The $(SU(3))^3$ Pseudogoldstone Model

We consider a supersymmetric grand unified model based on the gauge group $G \equiv SU(3)_c \times SU(3)_L \times SU(3)_R$. The matter (lepton, quark, antiquark) fields of the model transform as $(1, \bar{3}, 3)$, $(3, 3, 1)$ and $(\bar{3}, 1, \bar{3})$ under G :

$$\begin{aligned}
\lambda_i &\equiv \begin{pmatrix} H_1 & H_2 & L \\ e^c & \nu^c & N \end{pmatrix}_i \\
Q_i &\equiv \begin{pmatrix} u \\ d \\ g \end{pmatrix}_i \\
Q_i^{(c)} &\equiv (u^c \ d^c \ g^c)_i, i = 1, 2, 3
\end{aligned} \tag{1}$$

The superfields H_1, H_2, L are $SU(2)_L$ doublets, where $SU(3)_L$ ($SU(3)_R$) acts along the columns (rows) of the matrices in (1). Under $SU(2)_L \times U(1)$, H_{1i}, H_{2i} have the same quantum numbers as the EW doublets, while L_i denote the lepton doublets.

In order to break the gauge group G down to MSSM, we need higgs superfields that transform as the λ_i 's in (1). The minimum number that is needed is two which we denote as

$$\lambda(\bar{\lambda}) \text{ and } \lambda'(\bar{\lambda}') \tag{2}$$

The conjugate superfields $\bar{\lambda}$ and $\bar{\lambda}'$ are needed to preserve SUSY when G breaks to the standard model gauge group. The scalar components of $\lambda(\bar{\lambda})$ acquire large non-zero vevs along the $N(\bar{N})$ directions such that G breaks to $SU(3)_c \times SU(2)_L \times SU(2)_R \times U(1)_{B-L}$. With $\lambda'(\bar{\lambda}')$ acquiring large vevs along the $\nu^c(\bar{\nu}^c)$ direction, the resulting unbroken symmetry will be $SU(3)_c \times SU(2)_L \times U(1)$.

Let us begin by specifying the part of the superpotential that involves the chiral superfields $\lambda, \bar{\lambda}$:

$$W_\lambda = S(\lambda\bar{\lambda} - \mu^2) + a\lambda^3 + b\bar{\lambda}^3 \quad (3)$$

Here λ stands for λ_α^A , $\lambda^3 \equiv \epsilon_{ABC} \epsilon^{\alpha\beta\gamma} \lambda_\alpha^A \lambda_\beta^B \lambda_\gamma^C$ (*etc.*), and S denotes a gauge singlet field S . To see how the pseudogoldstone mechanism operates, consider a situation in which we include an analogous term $W_{\lambda'}$ for the λ' sector, but there is no $\lambda - \lambda'$ mixing [for details see Ref.[6]]. In this limit there appears a larger global symmetry (“pseudo-symmetry”)

$$G_{gl} = [SU(3)_c \times SU(3)_L \times SU(3)_R]_\lambda \otimes [SU(3)_c \times SU(3)_L \times SU(3)_R]_{\lambda'} \quad (4)$$

under which $W_\lambda + W_{\lambda'} + \text{h.c.}$ is invariant. It has been shown [5] that when G breaks to $SU(3)_c \times SU(2)_L \times U(1)$, there emerge a pair of ‘massless’ doublets with the quantum numbers of the EW higgs:

$$\begin{aligned} P &= L\langle \nu^c \rangle - H'_2 \langle N \rangle \\ \bar{P} &= \bar{L}\langle \bar{\nu}^c \rangle - \bar{H}'_2 \langle \bar{N} \rangle \end{aligned} \quad (5)$$

We observe that the H'_2 component of P has the correct quantum numbers to couple (at tree level) to the down quarks and the charged leptons. However, the corresponding component \bar{H}'_2 of \bar{P} cannot serve as the second (‘up’ type) higgs doublet since it is forbidden from having a renormalizable coupling to the quark superfields. In particular, the top quark is massless at tree level!

The resolution of this lies in extending the field content of the model by including an additional higgs supermultiplet $\lambda''(\bar{\lambda}'')$. Consider the superpotential couplings ($M \sim M_{GUT}$)

$$M\lambda''\bar{\lambda}'' + f\bar{\lambda}'\bar{\lambda}\bar{\lambda}'' \quad (6)$$

The second term in (6) explicitly breaks G_{gl} but in such a way that the desired ‘massless’ pair survives. A straightforward calculation shows that the combination

$$-\sin \alpha \ H_1'' + \cos \alpha \ \bar{P} \quad (7)$$

is the required ‘up-type’ higgs doublet. Here $\sin \alpha = z/(M^2 + z^2)^{1/2}$ ($z = f(N^2 + \nu^{c^2})^{1/2}$) provides a measure of the breaking of the pseudosymmetry G_{gl} .

In order to evaluate the scalar potential involving the EW higgs doublets, we turn attention to the relevant part of the superpotential

$$W = \Sigma_i (a_i S_i) P \bar{P} + \tilde{W}(S_i, \text{other fields}) + z \bar{P} \bar{H}_1'' + M H_1'' \bar{H}_1'' \quad (8)$$

where S_i denote the $SU(2) \times U(1)$ singlet superfields. The scalar mass² matrix, after including the soft supersymmetry breaking couplings, is given by (m_0 denotes the soft SUSY breaking scalar mass parameter and S_i in (9) and (10) denote the appropriate vev):

$$\begin{array}{ccccc} P^* & & \bar{P} & & \bar{H}_1''^* & H_1'' \\ \hline P & | a_i S_i |^2 + m_0^2 & a_i \frac{\partial \tilde{W}^*}{\partial S_i^*} + A a_i S_i & a_i S_i z & 0 \\ \bar{P}^* & a_i^* \frac{\partial \tilde{W}}{\partial S_i} + A a_i^* S_i^* & | a_i S_i |^2 + m_0^2 + z^2 & B z & M z \\ \bar{H}_1'' & a_i S_i z & B z & z^2 + M^2 & B M \\ H_1''^* & 0 & M z & B M & M^2 \end{array} \quad (9)$$

The presence of the ‘massless’ state (for $z = 0$) leads to the following relation

$$\begin{aligned}
|a_i S_i|^2 + m_0^2 &= a_i \frac{\partial \tilde{W}}{\partial S_i^*} + A a_i S_i \\
&= m_0^2 (b^2 + 1)
\end{aligned} \tag{10}$$

with $b = \frac{C-A}{2m_0}$, where A, B, C denote the common tri-linear, bi-linear and linear scalar couplings from the soft SUSY breaking at M_G . Note that $\langle S_i \rangle = 0 (= b m_0)$ before (after) SUSY breaking.

The 4×4 matrix in (9) can be simplified in a relatively straightforward manner and we will focus on the ‘light higgs’ sector which is given by the following 2×2 submatrix:

$$\begin{array}{ccc}
P^* & & H_u \\
\begin{matrix} P & m_0^2(b^2 \cos^2 \alpha + 1) & m_0^2(b^2 + 1) \cos \alpha \\ H_u^* & m_0^2(b^2 + 1) \cos \alpha & m_0^2(b^2 \cos^2 \alpha + 1) \end{matrix} & & (11)
\end{array}$$

where H_u stands for the state given in eq.(7).

The following remarks are in order:

- i. With $\alpha = 0$ the pseudosymmetry G_{gl} is unbroken at tree level in the scalar sector and we have a pair of ‘massless’ states with $\mu_1^2 = \mu_2^2 = \mu_3^2$ (at M_G).
- ii. The realistic case requires $\alpha \neq 0$ so that, at M_G ,

$$\begin{aligned}
\mu_1^2 &= \mu_2^2 = m_0^2(b^2 \cos^2 \alpha + 1) \\
\mu_3^2 &= m_0^2(b^2 + 1) \cos \alpha
\end{aligned} \tag{12}$$

The deviation from unity (at M_G) of the ratio $r (\equiv \sqrt{\mu_{1,2}^2/\mu_3^2})$, which can be significant as a consequence of (12), will be used in conjunction

with radiative electroweak breaking, to explore the parameter space of MSSM.

- iii. In minimal supergravity, $B = A - m_0$, $C = A - 2m_0$, such that $b = -1$.

3 Radiative Electroweak Breaking and $r \approx 1$

In this section we wish to explore how close to unity r can get without running into conflict with the radiative electroweak breaking scenario. For r sufficiently close to unity the well known parameter $\tan \beta$ turns out to be of order unity. The converse, however, is not necessarily true as we will later see. The procedure we follow rests on minimizing the renormalization group improved tree-level potential at a scale $Q_0 \sim 0.5 - 1 \text{ TeV}$. The soft SUSY breaking parameters at this scale are estimated through their one-loop evolution equations. The reliability of minimizing the tree-level potential in this manner has previously been studied [2] and yields results that are consistent with minimizing the one-loop effective potential.

A knowledge of α_s and the electroweak couplings at present energies enables us to estimate M_G through their one loop evolution equations, with supersymmetry breaking scale assumed to be of order Q_0 . By specifying h_t and $h_b (= h_\tau)$ at M_G , one evolves the coupled system for the gauge and third generation Yukawa couplings down to Q_0 , and solves for $\tan \beta$ from the known value of m_τ ($= 1.78 \text{ GeV}$). [We remark that in the $(SU(3))^3$ framework the asymptotic relation $h_b = h_\tau$ may be expected to hold near the Planck scale where the full E_6 theory is effective.] Furthermore, given $M_{1/2}$, m_0 and A one obtains the values of $m_{H_2}^2$ and $m_{H_1}^2$ at Q_0 , and from

the minimization conditions and knowledge of $\tan\beta$, solves for $\mu(Q_0)$ and $B(Q_0)$. [Note that at one-loop level, μ and B do not enter the evolution equations of the remaining parameters.] Knowing $\mu(Q_0)$ and $B(Q_0)$, we can compute the physical spectrum since the remaining parameters are already known via their evolution equations. If the result is a consistent, stable $SU(2) \times U(1)$ breaking vacuum [one that does not conflict any phenomenological constraint] we evolve $\mu(Q_0)$ and $B(Q_0)$ back to M_G and evaluate the parameter r . The procedure we follow gives results that are within $1 - 2\%$ of a one-loop calculation [7] which explicitly reports the values of $\mu(M_X)$ and $B(M_X)$ in order to implement a successful radiative breaking scenario.

We have performed a search in the parameter space spanned by

$$(h_t, h_b, M_{1/2}, m_0, A) \quad (13)$$

fixing $M_G \simeq 2 \times 10^{16}$ GeV, $Q_0 \sim 350$ GeV, $\alpha_s(M_Z) = 0.12$, $\alpha_G = 1/25$ ($\alpha_{em}(M_Z) = 1/128$). We illustrate the behaviour of the solutions in the desired regions of the parameter space through several figures to bring out the salient features. We begin by specifying a convention in which the Yukawa couplings, $M_{1/2}$ and $\tan\beta$ are positive, allowing A and μ to be of either sign. We shall see that if r is to be as close to unity as possible, the parameters A and μ will be required to have a common sign. [The qualitative trends are similar when $\mu, A < 0$ is replaced by $\mu, A > 0$.] In particular, the hierarchy which emerges, $M_{1/2} \ll m_0 \ll |A|$, favours the sign of A to be $+(-)$ when $\mu > 0(< 0)$. The numerical choices for (13) correspond to those that yield phenomenologically acceptable solutions often lying in the ranges reviewed in Ref. [2]. Such solutions are typical and the gross features

of the solutions are perturbed in only a minor way when these are modified.

In Fig. 1 we illustrate the dependence of r on $\tan \beta$, varying the input value of $h_t(M_G)$. Notice that as h_t increases it becomes harder to achieve $r \approx 1$.

In Fig. 2 we illustrate the correlation between the input value of A with the value of the parameter r . Here we have chosen $\mu < 0$ and one finds that $A = -3m_0$ makes r close to unity than say $A = -2m_0$, with all other parameters held fixed. [For $\mu > 0$, it is $A = 3m_0$ versus say $A = 2m_0$.] Thus the requirement of $r \approx 1$ favors a larger ratio for $|A|/m_0$.

In Fig. 3, we show the correlations between $M_{1/2}$ and m_0 when r is plotted as a function of $\tan \beta$ for differing ratios $m_0/M_{1/2}$. The net conclusion to be drawn is that the $r \approx 1$ scenario enforces the correlation

$$M_{1/2} \ll m_0 \ll |A| \quad \text{and} \quad \text{sign}(A) = \text{sign}(\mu) \quad (14)$$

In Fig. 4 we further develop the message found in Fig. 1 for larger values of h_t , with $M_{1/2}/m_0$ and A/m_0 in the regimes singled out by the scenario, to estimate how close to unity r can get. We see that to obtain $r \approx 1.05$ with $\mu < 0$ one requires m_0 to be as large as $2M_{1/2}$. Note that if $\tan \beta$ is too close to unity, the relation

$$m_t(m_t) = h_t(m_t)(174) \sin \beta \quad (15)$$

may cause the top quark mass in the theory to come into conflict with the CDF/D0 values [8].

With $\mu > 0$ a plot of r as a function of $\tan \beta$ is illustrated in Fig. 5.

The results above essentially emerge due to the correlations enforced by the well known evolution equations for the parameters μ and B [see Ref. 9] and are given here for completeness:

$$\begin{aligned} \frac{d\mu}{dt} &= \frac{\mu}{16\pi^2} \left(-3g_2^2 - \frac{3}{5}g_1^2 + h_\tau^2 + 3h_b^2 + 3h_t^2 \right) \\ \frac{dB}{dt} &= \frac{1}{8\pi^2} \left(-3g_2^2 M_2 - \frac{3}{5}g_1^2 M_1 + h_\tau^2 A_\tau + 3h_b^2 A_b + 3h_t^2 A_t \right) \end{aligned} \quad (16)$$

where $t = \log Q/M_X$.

So far we have considered the variation of r as a function of $\tan \beta$ in a region where $m_t(m_t)$ depends linearly on $\sin \beta$, namely where $h_b (= h_\tau) \ll h_t$ and is therefore neglected. Nevertheless, as $\tan \beta$ increases, h_b begins to grow in relative importance and eventually plays a role in arresting the growth of $m_t(m_t)$ as $\tan \beta$ grows for fixed h_t , eventually causing it to turn around. This is the reason why the quasi ‘infrared fixed point’ prediction for m_t (with $\tan \beta \simeq m_t/m_b$) is significantly smaller than the corresponding prediction with $\tan \beta \simeq 1$. For each value of h_t , with the favoured hierarchy corresponding to $r \approx 1$, one can plot r as a function of $m_t(m_t)$. The result is presented in Fig. 6 describing the correlation between $m_t(m_t)$ and r . The cross-over for the two contours $h_t = 2$ and 1 shows that, provided the top is heavy enough, merely lowering h_t will not suffice to enforce r in the vicinity of unity. Furthermore, from the preceding discussion, with $h_t = 1$ one cannot have a top quark heavier than 182 GeV.

The conclusion to be desired from Fig. 6 is that should the top weigh more than 180 GeV, $r \lesssim 1.12$ would be ruled out. If $m_t(m_t) \gtrsim 191$ GeV,

we would be forced to have $h_t(M_G) \gtrsim 2$ and $r \gtrsim 1.24$. In this region the infrared prediction begins to be realized, whereby ever larger $h_t(M_G)$ would be implied with a rapidly increasing lower bound on r . We also note here that with $\tan \beta \simeq 1.2$ and with the choice of parameters of Fig. 6, the $r \approx 1$ solution also satisfies the boundary condition of the ‘minimal’ Kähler model, viz., $B = A - m_0$.

The main result to be drawn from Figs. 1-6 is that with r sufficiently close to unity, the hierarchy $M_{1/2} \lesssim m_0 \lesssim |A|$ is singled out. In particular for r sufficiently close to unity (≤ 1.15), one finds that $1 \lesssim \tan \beta \lesssim 5$.

It is reasonable to enquire if the ‘small’ (order unity) $\tan \beta$ region requires that r also be close to unity. This turns out to be not the case. In Figs. 7a,b,c we show plots of r versus A/m_0 for a typical choice of $M_{1/2}$, m_0 and h_t , with $\tan \beta$ varying between ‘order unity’ to ‘intermediate’ values. The parameter $\mu > 0$. We see from 7b, for instance, that r can be large with $\tan \beta = 3$. This is a result of the fact that the parameter $B(M_G)$ estimated through its one-loop evolution equation suffers a change in sign as the ratio A/m_0 is varied from its phenomenologically allowed lower bound of -3 for such values of $\tan \beta$. For smaller values of $\tan \beta$, for instance 1.2, such a sign shift occurs at values of this ratio smaller than -3, which are phenomenologically excluded. Furthermore, in order to demonstrate that these features are not a result of accidental correlations between the input parameters, we present in Figs. 8 and 9 systematic studies of the variations of r as a function of A/m_0 for differing choices of input parameters. These trends persist if $\mu < 0$ and $A/m_0 \rightarrow -A/m_0$. An example is presented in Fig. 10.

4 Large $\tan \beta$ versus r

The phenomenological considerations are somewhat different in the event of large $\tan \beta$ since the effects of h_b and h_τ are no longer negligible which tends to make the lighter stau approach the mass of the LSP. Naturally we require this scalar tau to be heavier than the LSP. Furthermore, in this limit, due to the essential degeneracy of $m_{H_1}^2$ and $m_{H_2}^2$, m_A also tends to remain low. In fact in the limit that $\tan \beta \approx m_t/m_b$, such considerations play a crucial role in constraining regions of the parameter space[11]. It is no longer possible to choose m_0 to be (much) larger than $M_{1/2}$, and the ratio A/m_0 is also forced to remain rather low. We have performed a search in the parameter space to minimize r under these conditions. The result is displayed in Fig. 11. Here we present the variation of $\tan \beta$ with r , obtained by varying $h_b (= h_\tau)$ from $0.5h_t$ to h_t , with h_t chosen to be sufficiently large ($=1.5$), such that $m_t(m_t)$ lies between 185 and 181 GeV . The universal gaugino mass $M_{1/2}$ is chosen to be 800 GeV (and $Q_0 \sim 1 TeV$) in order to saturate the upper bound on the (bino-like) lightest neutralino mass of 350 GeV . For this figure we obtain the minimum value of r with $\mu > 0$, with the maximum realizable values of m_0 and the ratio A/m_0 consistent with the phenomenological requirements $m_A \geq m_Z$ and $m_{\tilde{\tau}_1} \geq m_{\tilde{N}}$. What we find is that r cannot be smaller than about 1.5 as we near the condition of exact Yukawa unification ($h_t = h_b = h_\tau$ at M_G). Indeed if the exact Yukawa unification condition is relaxed, there is considerable freedom in the ratio A/m_0 as well, and even in the large $\tan \beta$ case r can be just about as large as one wants like in the ‘intermediate’ $\tan \beta$ case.

5 Conclusions

The idea that the electroweak higgs doublets of MSSM may arise as ‘pseudogoldstones’ of an underlying supersymmetric grand unified theory can be neatly realized within the framework of $SU(3)_c \times SU(3)_L \times SU(3)_R$. In this work we have studied the implications when this idea is merged with that of radiative electroweak breaking. In particular, we have explored the constraints on the ‘universal’ parameters $M_{1/2}$, m_0 and A . An important lesson is that the low energy parameter $\tan \beta$ can vary all the way from order unity to m_t/m_b in this class of models. Depending on the top quark mass, certain lower bounds on the parameter r have been identified.

Acknowledgements

We thank Gia Dvali for important discussions on the pseudogoldstone phenomenon in SUSY GUTS. B.A. thanks the Swiss National Science Foundation for support during the course of this work. The work of Q.S. is supported in part by the US Department of Energy, Grant No. DE-FG02-91 ER 40626.

Note Added

The results of this paper were briefly discussed at the SUSY '95 meeting in Paris and at the “European High Energy Physics” conference in Brussels. After this paper was completed we came across a recent paper by C. Csáki and L. Randall (hep-ph/9512278) in which similar ideas are discussed. Where our work overlaps the results are in broad agreement.

References

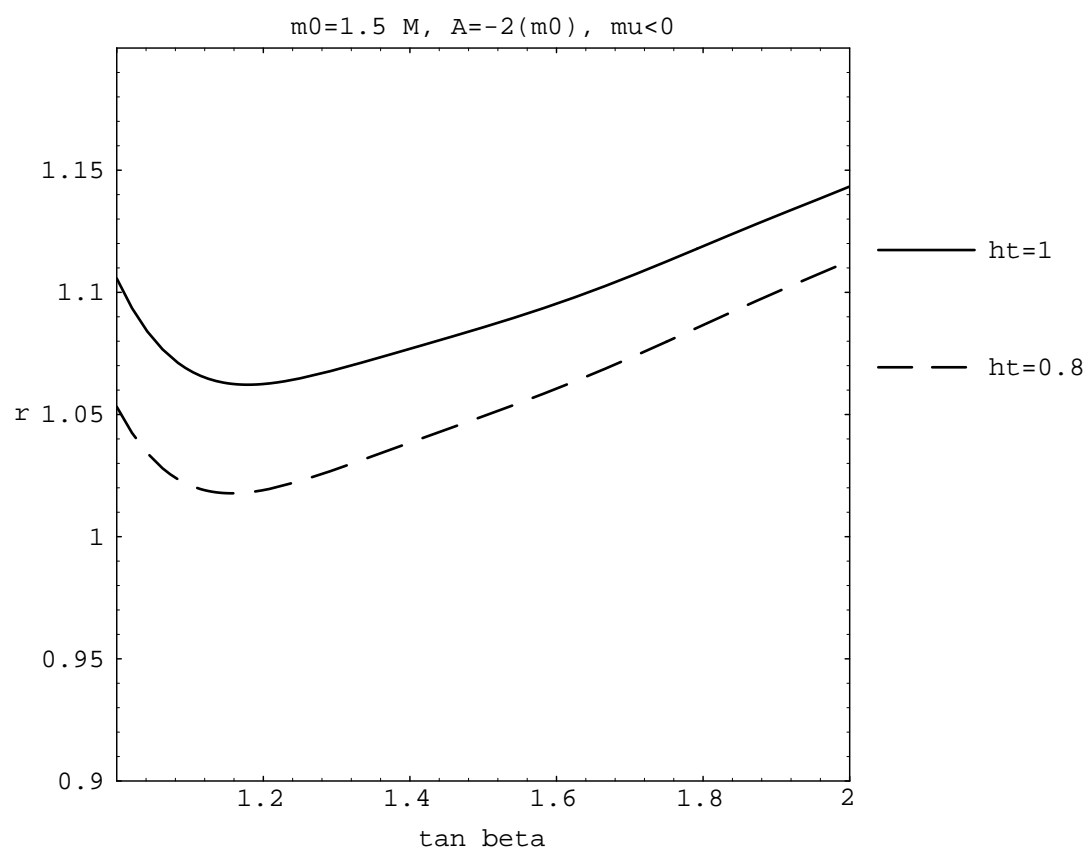
- [1] G. Dvali and Q. Shafi, Phys. Lett. B 326 (1994) 258; ibid 339 (1994) 241.
- [2] B. Ananthanarayan, G. Lazarides and Q. Shafi, Phys. Rev. D 44 1613 (1991); for a recent review with additional references, see B. Ananthanarayan and Q. Shafi, “Predicting the top quark, sparticle and higgs masses in supersymmetric grand unified models,” Proc. of the 2nd I.F.T. Workshop on Yukawa Couplings, P. Ramond ed., International Publishing House, Boston, USA (1994).
- [3] K. Inoue, A. Kakuto and T. Takano, Prog. Th. Phys. 75 (1986) 664; A. Anselm and A. Johansen, Phys. Lett. B200 (1988) 331.
- [4] Z. Berezhiani and G. Dvali, Sov. Phys. Lebedev Inst. Rep. 5 (1989) 55; R. Barbieri, G. Dvali and M. Moretti, Phys. Lett B 312 (1993) 137; Z. Berezhiani, C. Csaki and L. Randall, hep-ph/9501336 (1995); For a recent review see Z. Berezhiani, hep-ph/9503366 and references therein.
- [5] G.F. Guidice and E. Roulet, Phys. Lett. B 315 (1993) 107.
- [6] G. Dvali and Q. Shafi, Bartol preprint BA-94-42.
- [7] M. Bando, et al., Mod. Phys. Lett. A7 (1992) 3379.
- [8] S. Abachi et al., D0 Collaboration, Phys. Rev. Lett. 74 (1993) 2422.

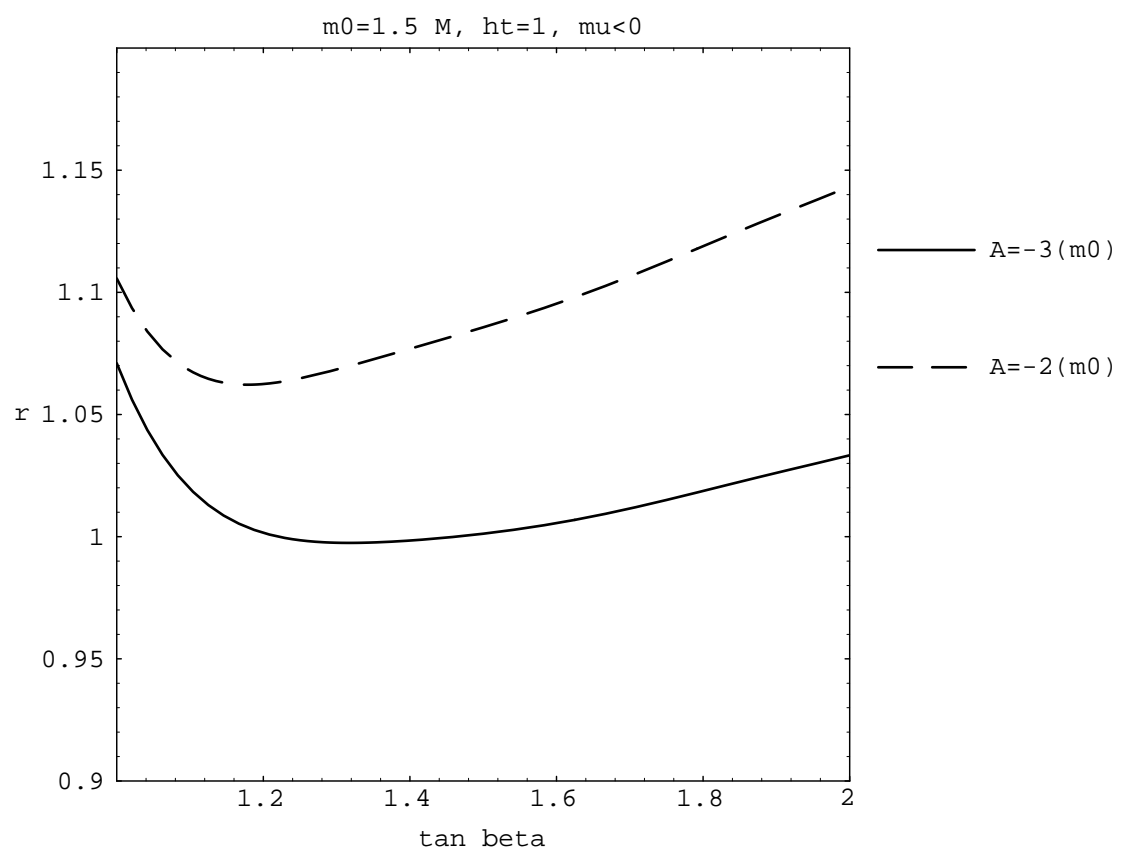
- [9] See for instance M. Drees and M. M. Nojiri, Nucl. Phys. B359 (1992) 54.
- [10] B. Ananthanarayan, K.S. Babu and Q. Shafi, Nucl. Phys. B428 (1994) 19; M. Carena et al., Nucl. Phys. B369 (1992) 33.
- [11] B. Ananthanarayan, G. Lazarides and Q. Shafi, Phys. Lett. B 300 (1993) 245; B. Ananthanarayan, Q. Shafi and X-M. Wang, Phys. Rev. D50 (1994) 5980.

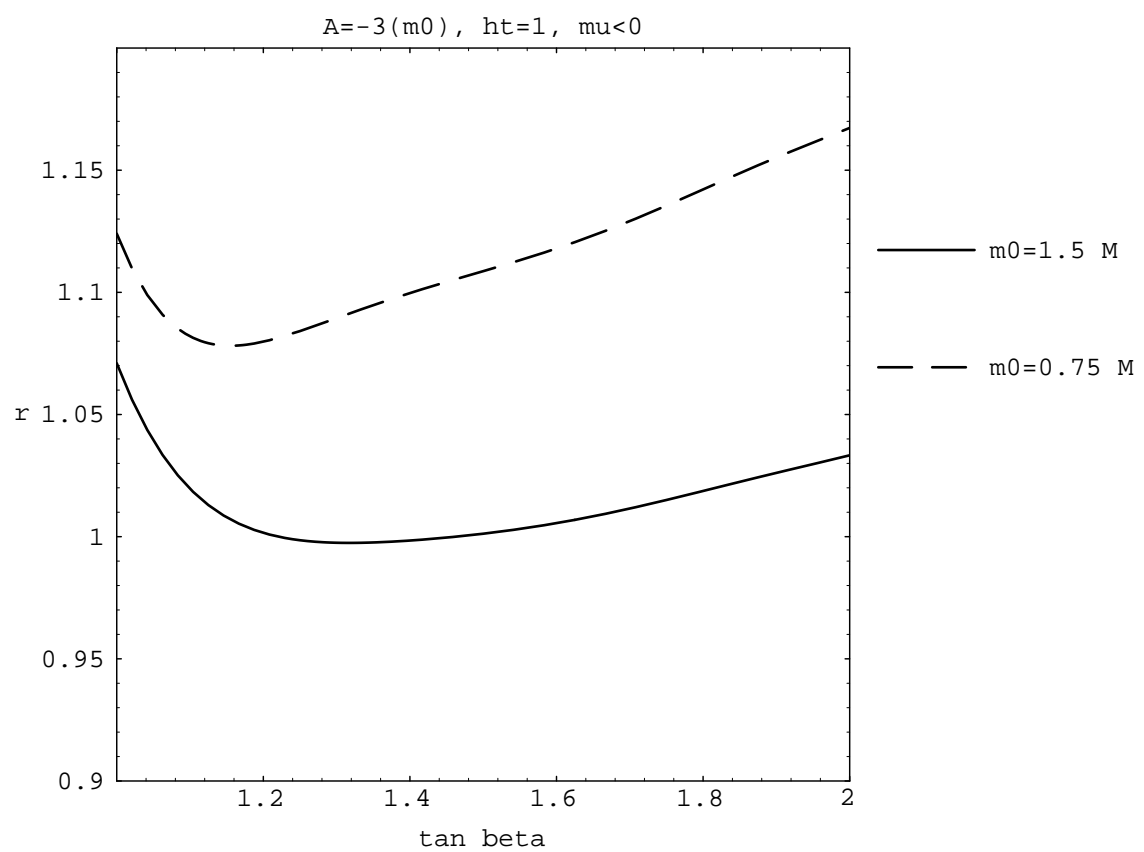
Figure Captions

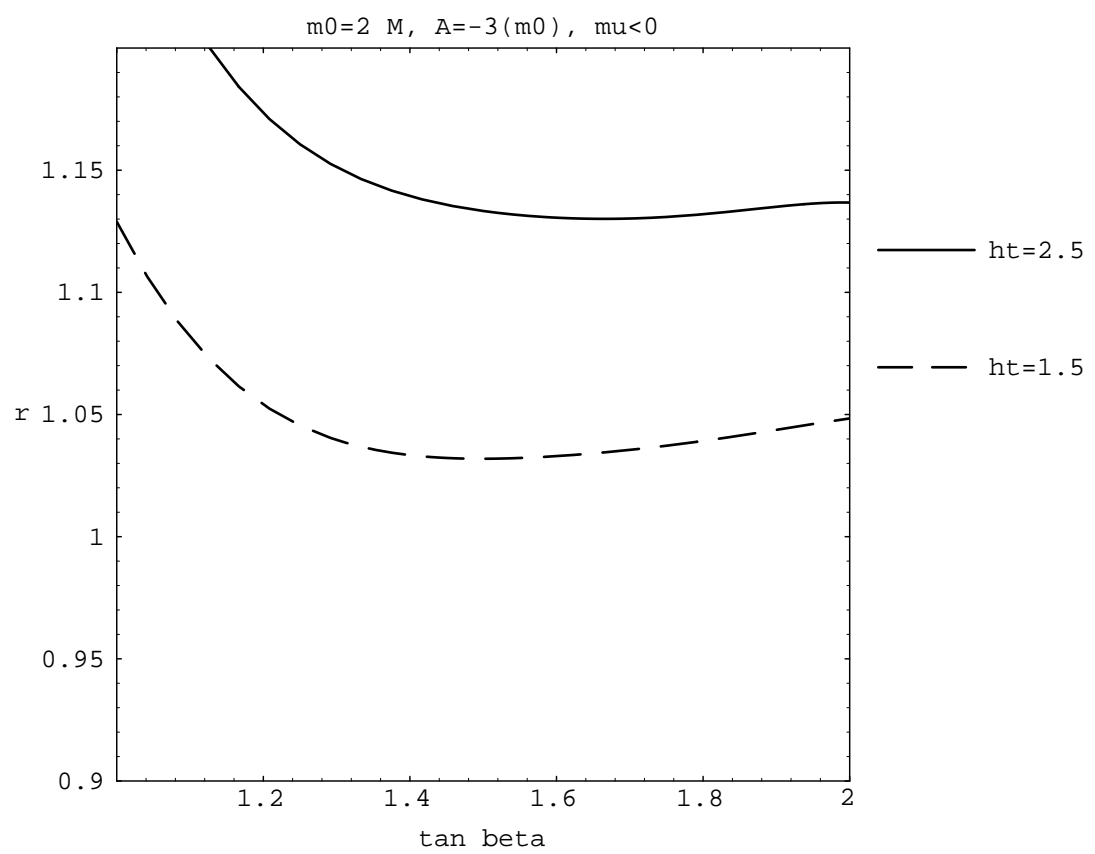
1. Plot of r versus $\tan\beta$ for $h_t = 1$ and 0.8 , with $m_0 = 1.5M_{1/2}$, $A = -2m_0$, $\mu < 0$
2. Plot of r vs. $\tan\beta$ for $A = -3m_0$ and $-2m_0$, with $m_0 = 1.5M_{1/2}$ and $h_t = 1$, $\mu < 0$
3. Plot of r vs. $\tan\beta$ for $m_0 = 1.5M_{1/2}$ and $0.75M_{1/2}$, with $A = -3m_0$ and $h_t = 1$, $\mu < 0$
4. Plot of r vs. $\tan\beta$ for $h_t = 2.5$ and 1.5 , $m_0 = 2 M_{1/2}$ and $A = -3 m_0$, $\mu < 0$
5. Plot of r vs. $\tan\beta$ for $h_t = 1.5$, $M_{1/2} = 270\text{GeV}$, $m_0 = 340\text{GeV}$ for $A = -3m_0$, $\mu < 0$ and $A = 3 m_0$, $\mu < 0$
6. Plot of r vs. $m_t(m_t)$ for $h_t = 1, 2, 3$, $M_{1/2} = 270\text{GeV}$, $m_0 = 340\text{GeV}$, $A = 3m_0$, $\mu > 0$.
7. (a) Plot of r vs. A/m_0 , for $M_{1/2} = 280\text{GeV}$, $m_0 = 340\text{GeV}$, $h_t = 2.5$, $\tan\beta = 1.2$, $\mu > 0$, (b) As in (a) with $\tan\beta = 3.0$, and (c) as in (a) with $\tan\beta = 7.8$.
8. As in Fig. 7 with $m_0 = 170\text{GeV}$.
9. As in Fig. 7 with $M_{1/2} = 420\text{GeV}$ and $m_0 = 510\text{GeV}$.
10. As in Fig. 9c with $\mu < 0$.

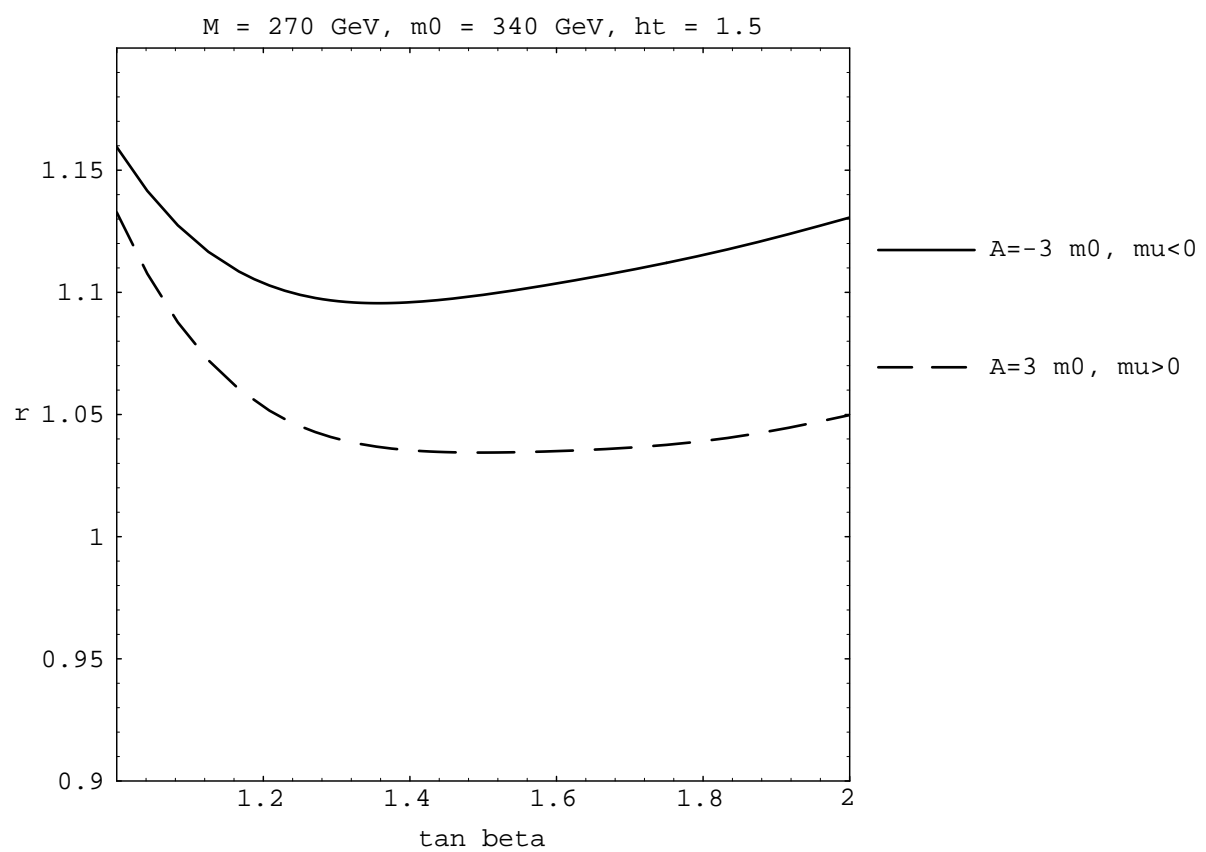
11. Plot of r vs. $\tan \beta$ in the large $\tan \beta$ regime with m_0 and A/m_0 chosen optimally so as to minimize r and saturate the requirement that $m_A \geq m_Z$ and $m_{\tilde{t}_1} \geq m_{\tilde{N}}$.

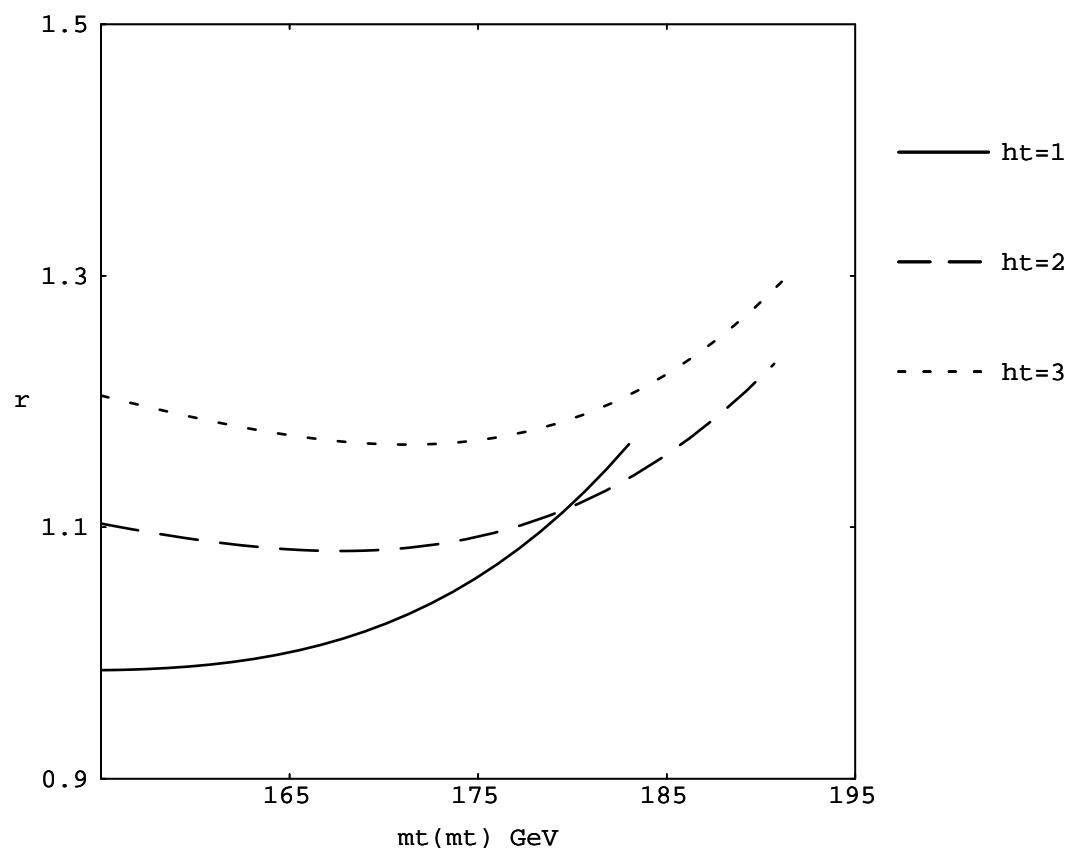




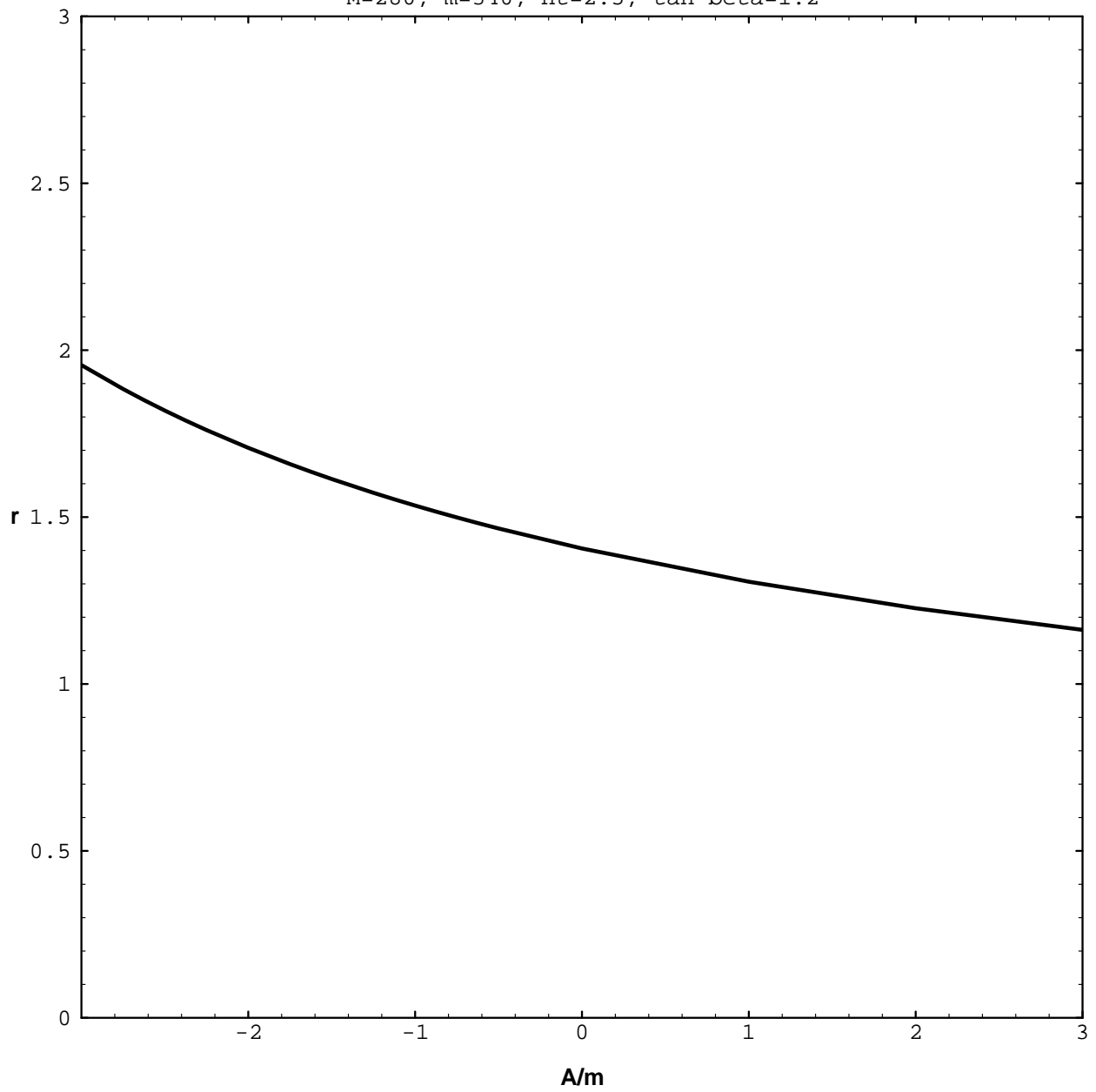




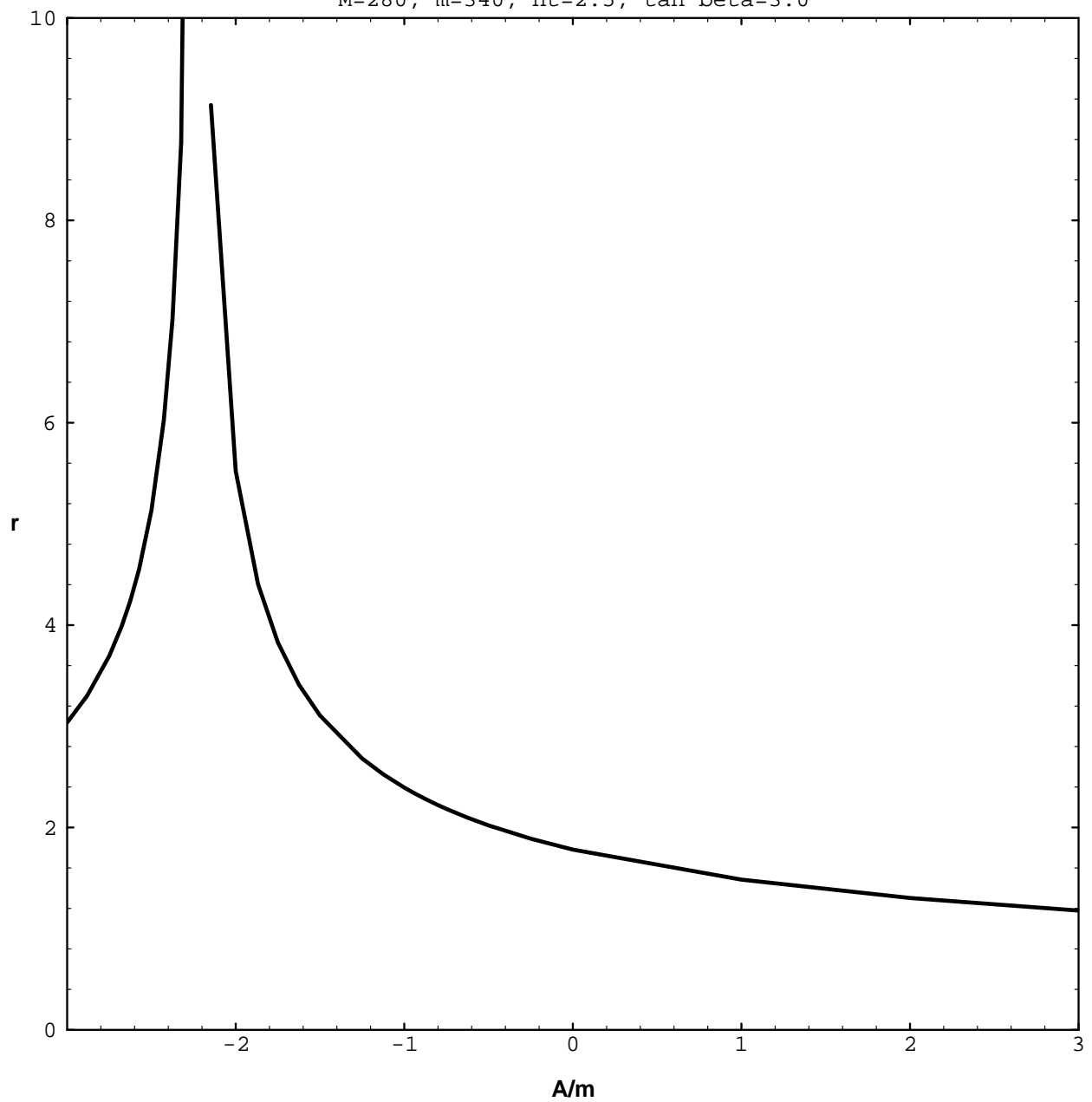




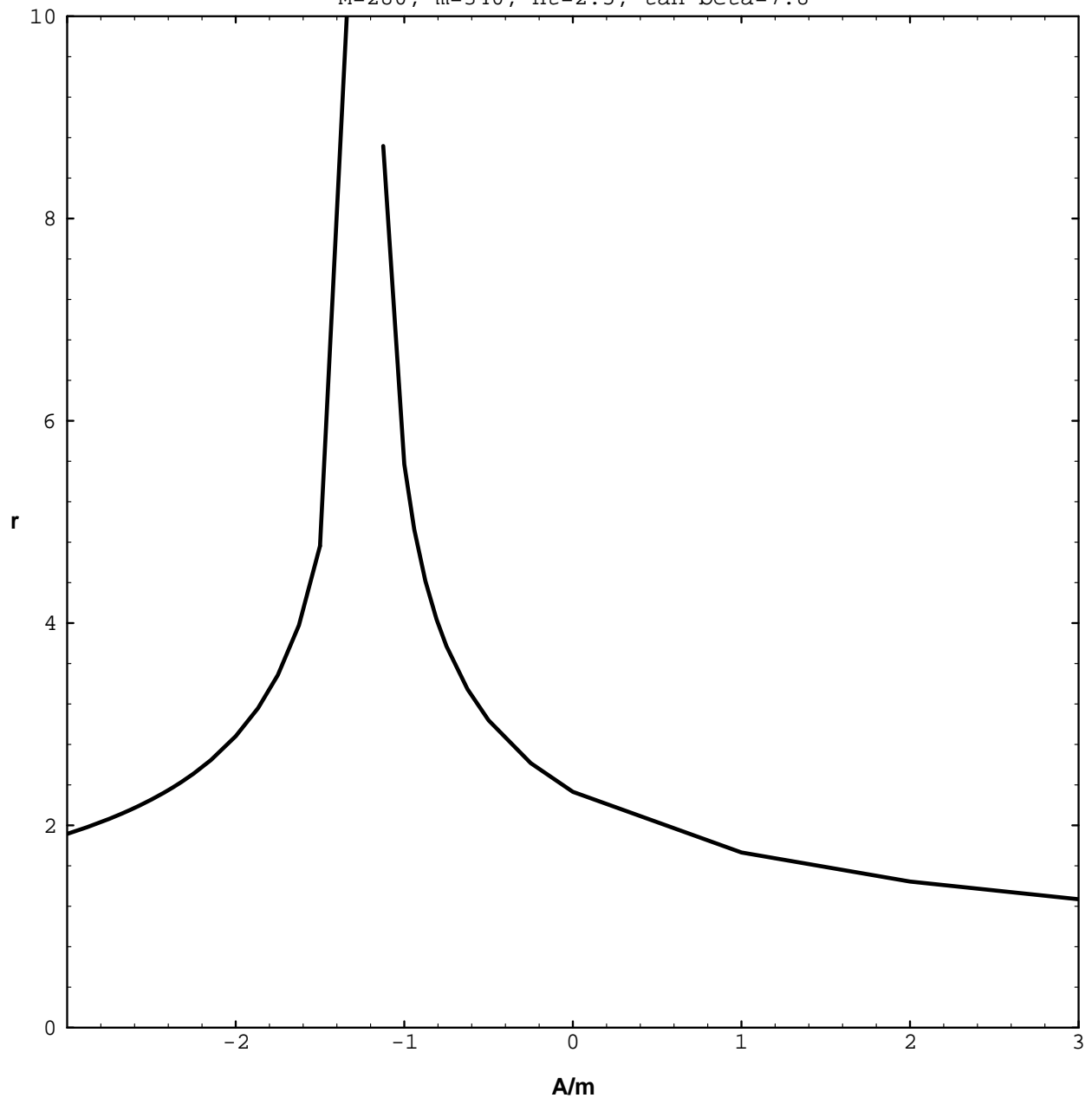
M=280, m=340, ht=2.5, tan beta=1.2



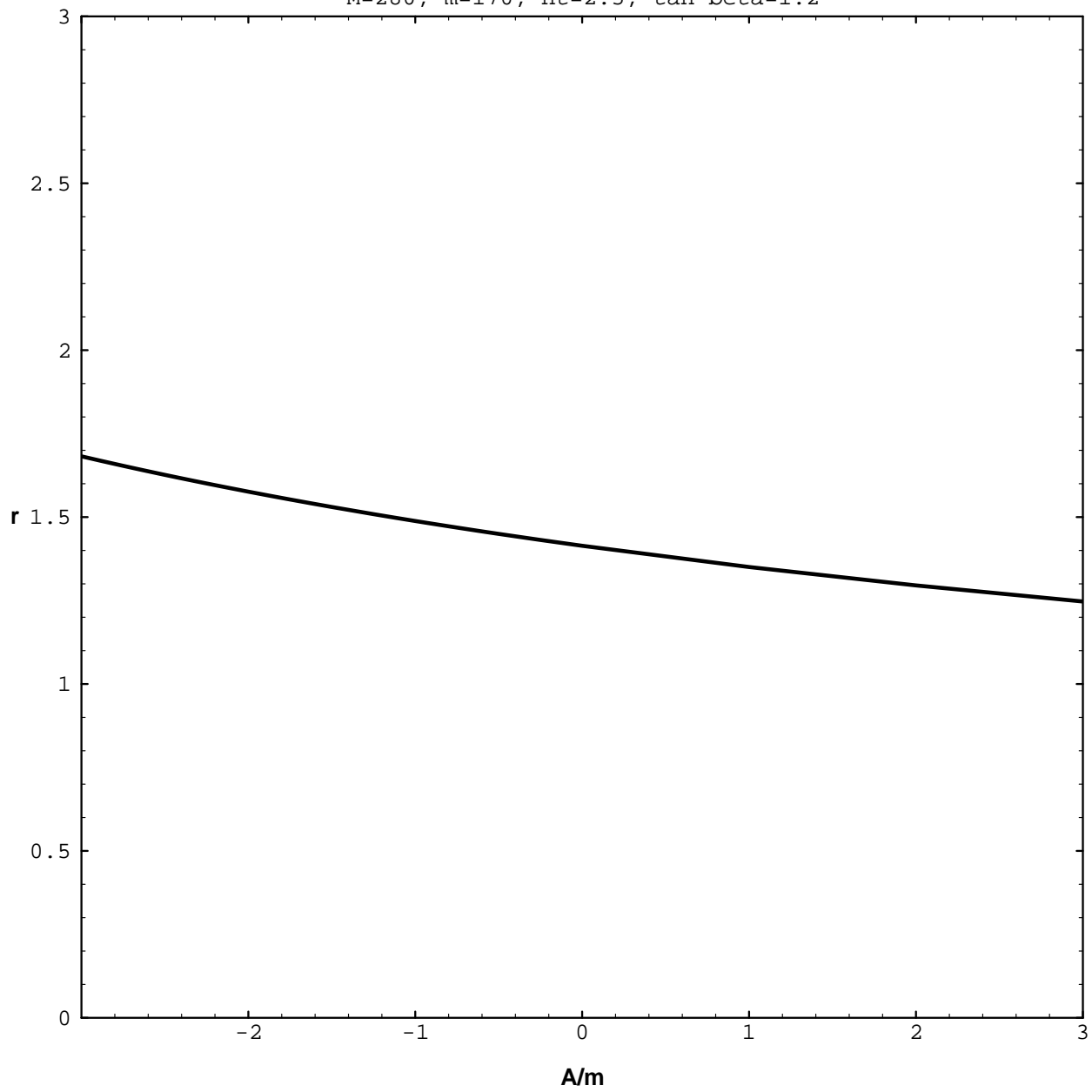
$M=280, m=340, ht=2.5, \tan \beta=3.0$



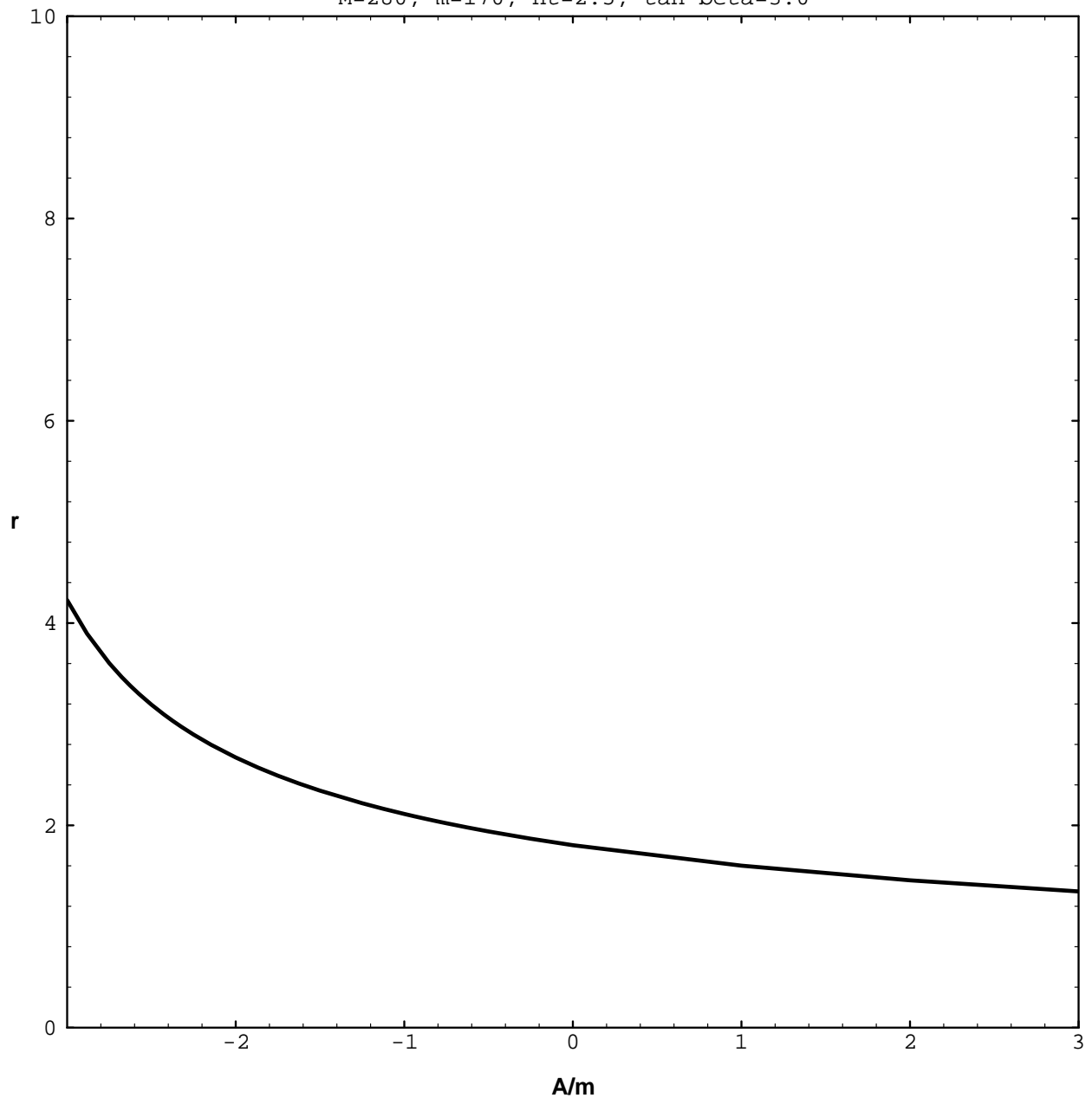
$M=280, m=340, ht=2.5, \tan \beta=7.8$



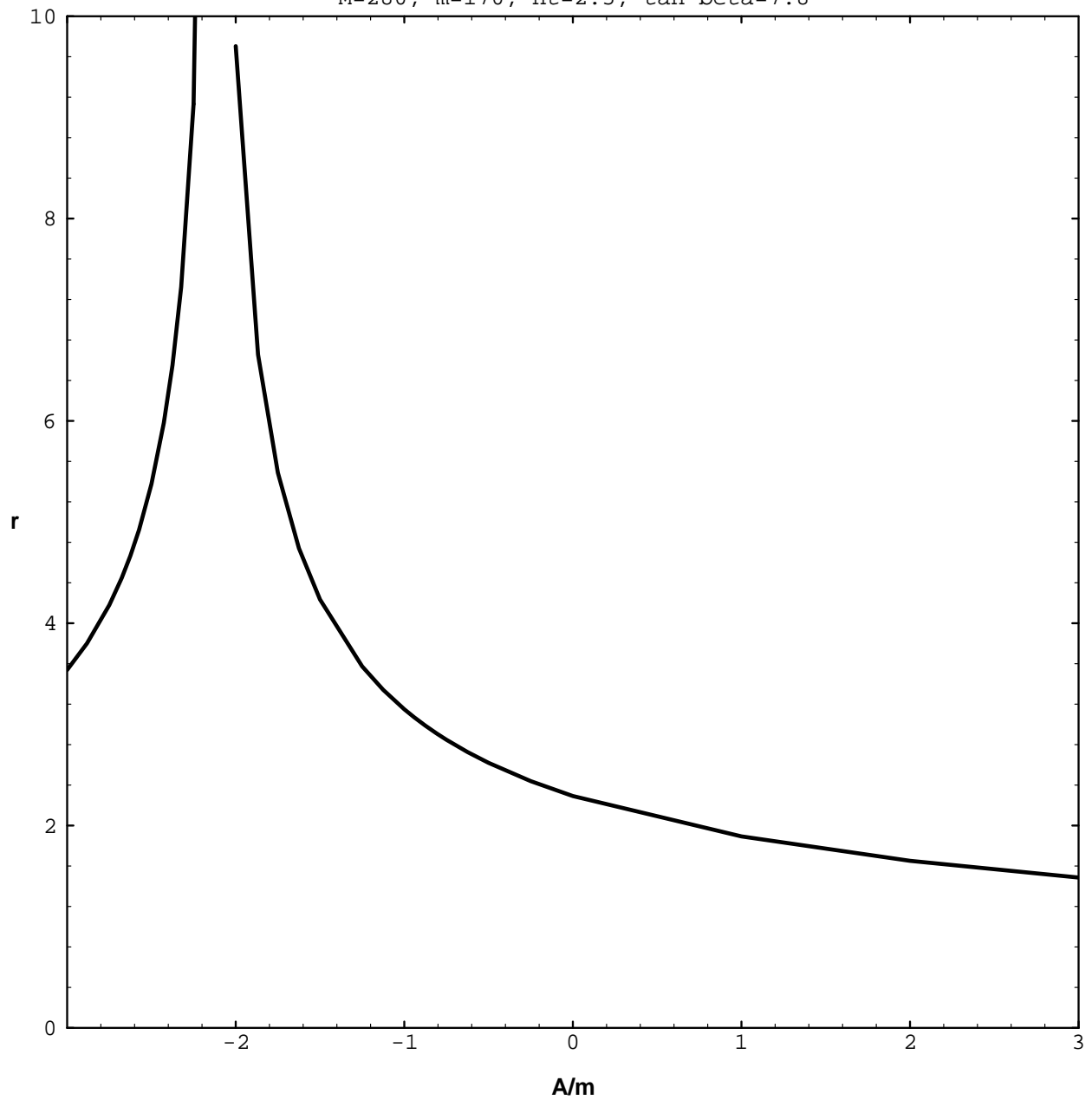
M=280, m=170, ht=2.5, tan beta=1.2



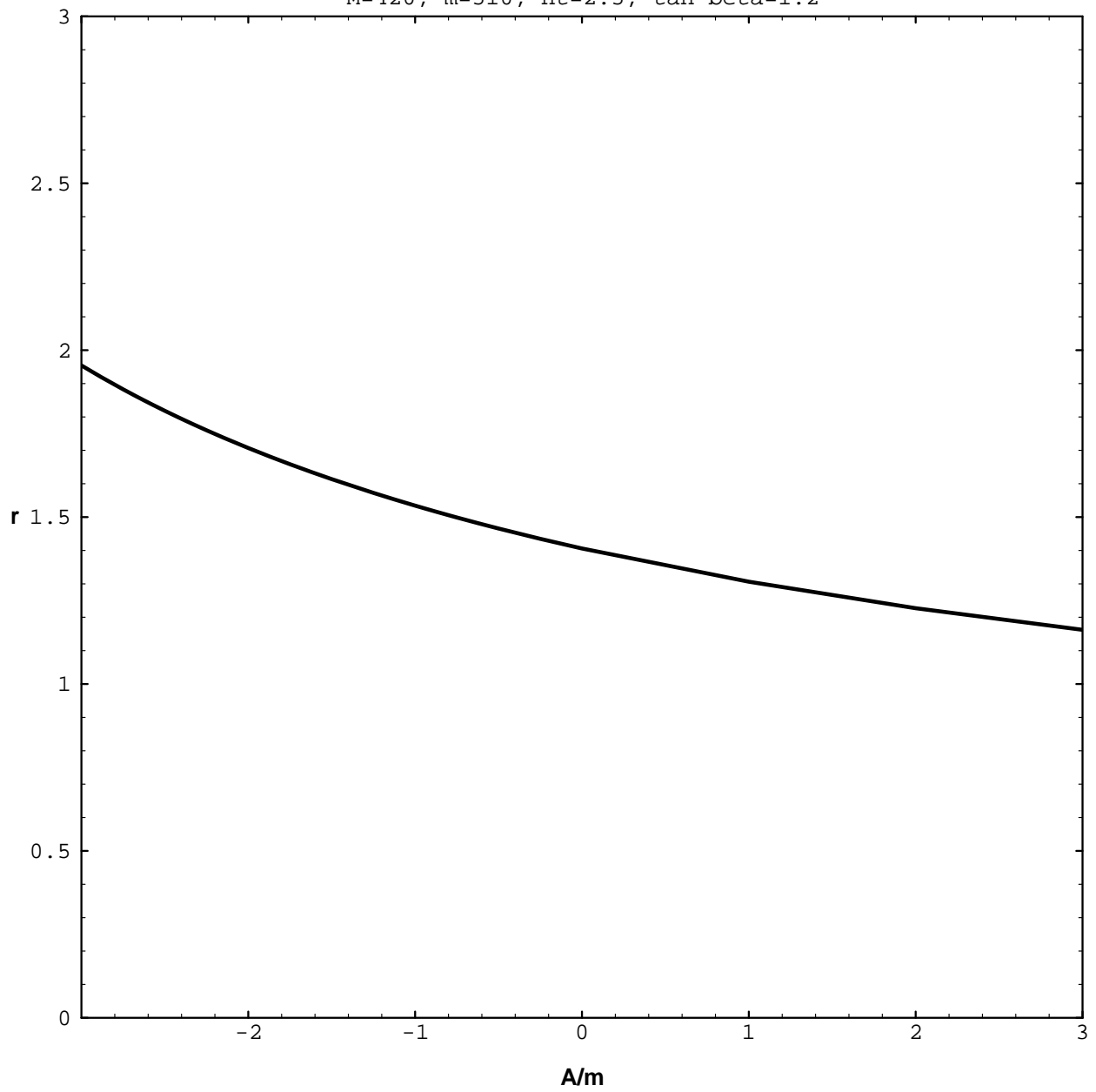
$M=280, m=170, ht=2.5, \tan \beta=3.0$



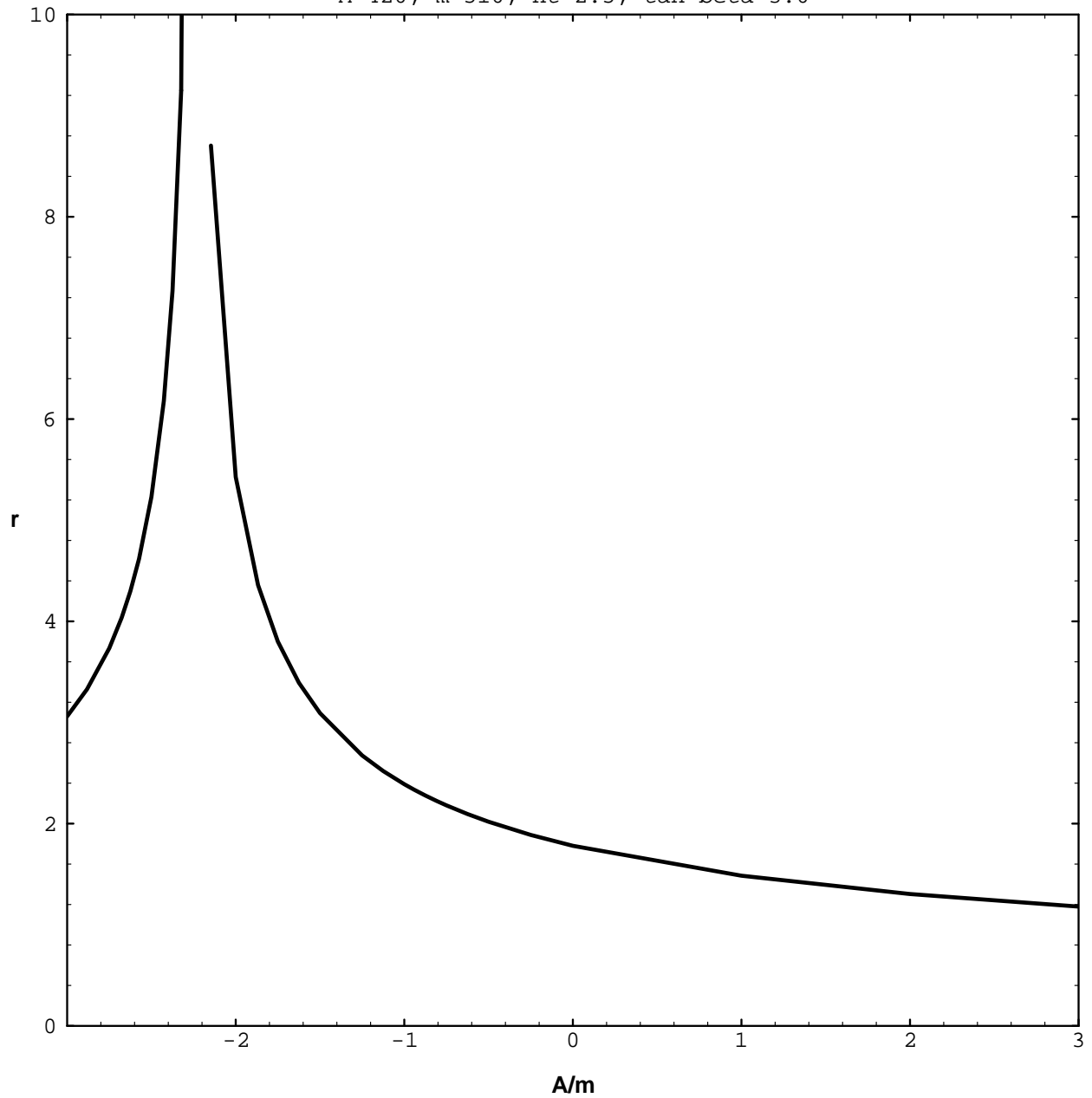
$M=280, m=170, ht=2.5, \tan \beta=7.8$



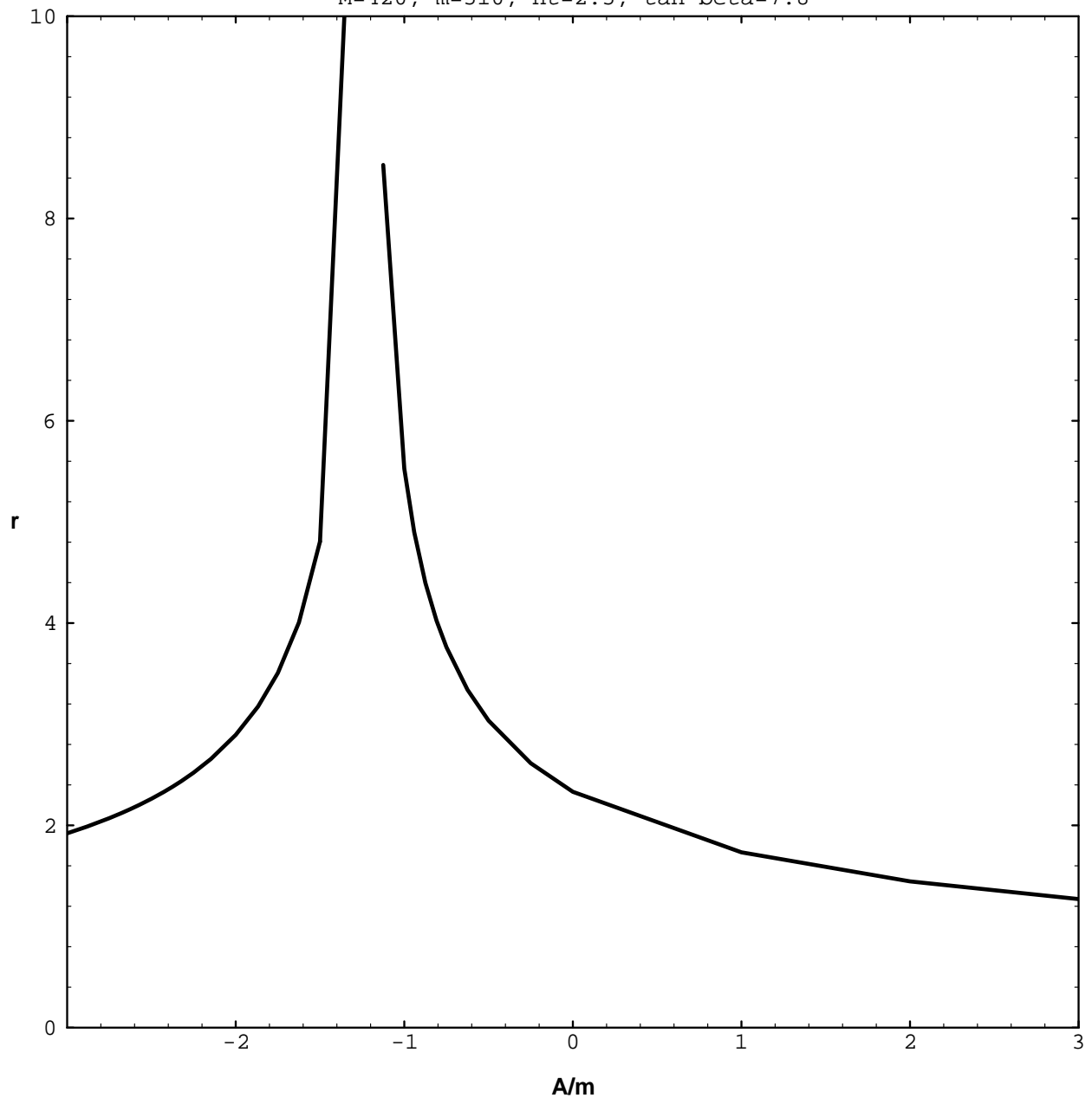
M=420, m=510, ht=2.5, tan beta=1.2



$M=420, m=510, ht=2.5, \tan \beta=3.0$



$M=420, m=510, ht=2.5, \tan \beta=7.8$



$M=420, m=510, ht=2.5, \tan \beta=7.8, \mu < 0$

